# Capillary Condensation due to van der Waals Attraction in Wet Slits

H. K. Christenson

*Department of Applied Mathematics, Research School of Physical Sciences, Australian National University, Canberra Australian Capital Territory 0200, Australia*

(Received 4 April 1994)

Wetting films (of thickness $t \leq 14$ nm) of $t$-butanol in slits of mica have been studied as a function of the slit width $H$. A capillary condensation transition occurs when $H \approx 3t$ for $t > 5$ nm. This is consistent with a mechanism of film thickening and coalescence due to van der Waals forces across the slit. van der Waals thickening cannot account for the transition with thinner ($t < 5$ nm) adsorbed films, as found previously with nonwetting liquids.

PACS numbers: 68.15.+e, 68.45.−v

The thickness $t$ of an adsorbed film at an isolated solid surface depends on the chemical potential $\mu$ (or relative vapor pressure $p/p_0$) of the adsorbing species. The Lifshitz theory of van der Waals forces predicts that simple liquids as well as water wet mica, i.e., that $t$ increases without bounds as saturation ($\mu = \mu_0$) is approached. By contrast, ellipsometry studies show that at saturation $t$ for water and nonpolar liquids like cyclohexane on mica is limited to about 2 nm (a possible exception is $n$-pentane), in agreement with their small but finite contact angle (5°−10°) on mica [1,2].

In a system of two surfaces, or a *slit,* the film thickness $t$ depends not only on $\mu$ but also on the slit width $H$ [see Fig. 1(a)]. At sufficiently small values of $H$ the film thickness will be influenced by the presence of the second surface. At some critical value of $H$ the vapor phase is no longer stable and the slit will fill up with condensed liquid. This is an example of capillary condensation—a gas-liquid transition shifted from its bulk location in the phase diagram by the proximity of two surfaces [3–6]. Using the theory of van der Waals forces Derjaguin and Churaev obtained a relationship between the critical slit width $H_c$ and a corresponding critical film thickness $t_c$ at which the adsorbed films on the opposing surfaces become unstable, grow without bounds, and coalesce [6]. Density functional treatments of confined fluids based on van der Waals forces confirm this picture [4]. The film growth corresponds to the spinodal end point of the vapor branch of the adsorption isotherm. The equilibrium transition is given by a Kelvin-type equation and occurs for smaller $\mu$ and $t_c$. Differences between the slit width at which condensation occurs on approach and that at which capillary evaporation occurs on separation (the liquid branch) give rise to hysteresis and such phenomena have been the subject of much discussion [7].

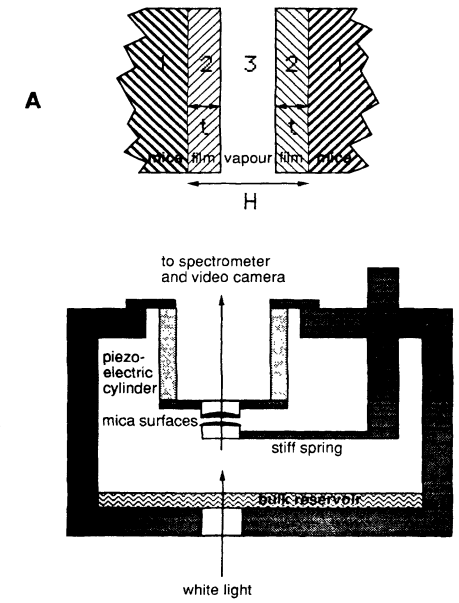


FIG. 1. Schematic depiction of (a) the "wet" slit and (b) the experimental setup.

The surface force apparatus [8] has been extensively used to study capillary condensation. The radius of meniscus curvature $r$ (for $r \geq 4$ nm) of capillary condensates around mica surfaces *in contact* has been found to agree with the Kelvin equation [9], viz.,

$$r = -\frac{\gamma v_m \cos\Theta}{kT \ln(p/p_0)}, \tag{1}$$

where $\gamma$ is the surface tension of the liquid, $\Theta$ its contact angle, and $v_m$ its molecular volume. Most experimental work on the formation of capillary condensates at *finite* slit widths has been carried out for the thermodynamically analogous case of water phase separating from its solutions in nonpolar liquids. The surfaces are pulled into contact from a finite separation due to the negative Laplace pressure in a condensate that forms on approach. A modified Kelvin equation, with the water activity $a_w$ replacing $p/p_0$ and the interfacial tension between water and nonpolar liquid $\gamma_i$ replacing $\gamma$ in Eq. (1), can be used to describe the condensation separation $H_c$ as a function of $a_w$ over a restricted range ($a_w = 0.7$–$0.95$) [10–12]. The limiting condensation separation at large $a_w$ depends on whether the mica is covered with hydrogen ions (9 nm) or potassium ions (13 nm). The type of surface ion

  

determines the short-range interaction between the mica surfaces across water; it is repulsive for potassium ions and attractive for hydrogen ions. The film-thickening model has recently been applied to this case but no agreement was obtained with the theory of van der Waals forces [13].

More recent experiments involving capillary condensation from vapor have shown that close to saturation the surfaces jump together at $H = 12 \pm 1$ nm as a capillary condensate is formed [14]. For $p/p_0 = 0.95-0.99$, where the ellipsometrically determined $t$ at isolated surfaces varies between 1 and 2 nm [1,2], $H_c$ is within error constant. The details of the process are too fast to be resolved within the time resolution of 20 ms (a video camera is used to record the interference fringes that yield the surface separation, refractive index, and surface shape). The film-thickening model fails to explain the condensation separations in ethanol vapor at $p/p_0 < 0.99$, where $t \leq 2$ nm [15].

A drop of ethanol placed on freshly cleaved mica [15] spreads to a film showing interference colors. Unlike cyclohexane or water, low-molecular weight alcohols wet mica, providing a suitable model system to study capillary condensation for thicker films. I have measured the condensation separation $H_c$ as a function of the adsorbed film thickness at this separation $t_c$ for mica slits in $t$-butanol vapor and compared the results to the predictions of the film-thickening model. $t$-butanol (2-methyl-2-propanol) was chosen because it does not attack the epoxy resin used to glue the mica surfaces to supporting silica discs.

With the surface force apparatus the separation between two curved ($R \approx 0.02$ m) surfaces of molecularly smooth mica can be controlled to within 0.1–0.2 nm using a piezoelectric device and measured with similar accuracy using multiple-beam interferometry (white light is passed through the system of back-silvered mica surfaces). The refractive index of the medium in the slit (between the mica surfaces) may be measured, and any surface deformations occurring as the result of strong interactions can be monitored. One of the surfaces is mounted on a spring of varying rigidity—in these experiments a stiff mount (spring constant $k \approx 5 \times 10^4$ N m$^{-1}$) was used. With a stiff spring only very large forces, such as those caused by condensation of liquid bridges between the surfaces, can be detected. The measured force $F(H)$ between curved surfaces of radius $R$ may be related to the free energy of interaction of parallel, flat surfaces $E(H)$ using the Derjaguin approximation, $F(H) = 2\pi RE(H), R \gg H$ [16]. In particular, this allows instabilities in the force (such as those causing inward jumps) to be related to instabilities in the free energy between flat surfaces.

The present experiments involve measuring the refractive index $n$ as a function of the slit width $H$ in $t$-butanol vapor. The thickness $t$ of adsorbed films of $t$-butanol may be calculated from $n$ and related to the measured $H_c$, at which the surfaces are pulled into contact. The experiments were carried out at 26 °C, just above the melting point of $t$-butanol of 25.5 °C [17]. The dielectric constant of $t$-butanol is low ($\varepsilon \approx 11$) and any ionization and consequent electrostatic interactions across the adsorbed films would be negligible. Even in methanol ($\varepsilon = 33$) double-layer forces are barely measurable [18]. By maintaining bulk $t$-butanol in the chamber [Fig. 1(b)] the system is kept close to coexistence but small deviations towards lower $p/p_0$ values are caused by a slight heating effect of the light beam as it passes through the back-silvered mica surfaces (despite three ir filters). The effective $p/p_0$ may be varied by leaving the surfaces apart with the light beam off for different times. The surfaces are brought to within 0.5 $\mu$m of each other, the light is switched on, and a video recording of the interference fringes as the surfaces are taken into contact is made. It was verified with a thermocouple that the temperature did not measurably change after the light was switched on during the time taken for such a recording (≈15 s). The measurement is hence taken at a constant temperature and thereby at a constant but unknown $\mu$ or $p/p_0$. The absence of contamination in the surface films of $t$-butanol was verified by checking that the films and capillary condensates evaporated when the light intensity was increased. Surface contamination leads to condensates that do not evaporate on decreasing the effective $p/p_0$ [10]. Water was eliminated by use of $CaH_2$ as a drying agent in the chamber.

The refractive index of the medium between the surfaces is a function of the wavelength shifts (measured from the videotapes using a videomicrometer) of two interference fringes of adjacent order [19]. Typical results of the measured refractive index $n$ as a function of $H$ are shown in Fig. 2, both when the chamber is filled with dry nitrogen only (filled circles) and $t$-butanol (open symbols). The two sets of data in $t$-butanol vapor show the difference

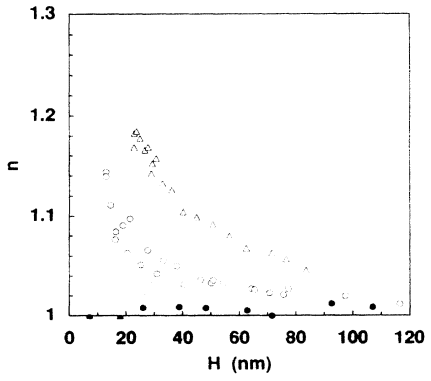


FIG. 2. Measured refractive index $n$ as a function of the separation between the mica surfaces (the slit width $H$) in nitrogen (filled circles) and $t$-butanol vapor (open circles and open triangles). The circles show data obtained with the light source left on for extended periods (hours); the triangles show data obtained during the first 15 sec after turning the light on (see text).

between when the light beam is on continuously and when it is left off for several hours before measuring, as described above. The accuracy of $n$ decreases considerably beyond about 100 nm, due to increasing nonlinearity of the video camera, which affects the accuracy of the measured wavelengths, as the position of one interference fringe gets close to the edge of the field of view.

For the layered system in Fig. 1(a) $n$ is related to the film thickness $t$ per surface and the surface separation $H$ by $nH = (H - 2t) + 2tn_f$ so that

$$t = \frac{H(n-1)}{2(n_f - 1)}, \tag{2}$$

where $n_f$ is the refractive index of the film (assumed equal to the bulk refractive index of $t$-butanol, 1.388) [20]. Some representative results are shown in Fig. 3, where the condensation separation is the point at the smallest $H$, where the surfaces are pulled into contact. The lines are least-squares fits to the data points for $H < 100$ nm. $t_c$ is taken to be the value of the fit at the measured separation $H_c$ (because $H$ can be more accurately determined than $t$). The thinner films ($t \leq 6$ nm) show a constant ($\pm 0.3$ nm) $t$ over the range of measured separations, but the thicker films (squares) show a small but noticeable ($\approx 2$ nm) increase in $t$ at smaller separations. For the thickest film ($t \approx 14$ nm, not shown), one observes how the films first coalesce ($n$ jumps discontinuously from 1.26 to 1.39 at $H_c$; i.e., $t$ jumps from $t_c$ to $H/2$) and then, one frame ($\approx 20$ ms) later, the surfaces are pulled together. With thinner films the coalescence and jump into contact are too fast to be resolved into separate events.

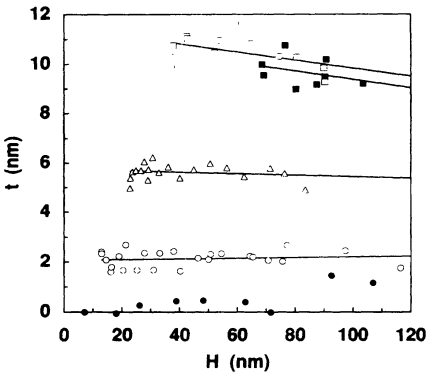


FIG. 3. Thickness $t$ of $t$-butanol films on either surface as a function of slit width $H$. The filled circles show the results in nitrogen (same data as in Fig. 2); the open circles and triangles are the same runs as shown in Fig. 2. The squares are the results of a run not shown in Fig. 2. The filled squares are the results on first approach; the surfaces were then separated $\approx 600$ nm and the open squares were obtained as the surfaces were brought together again. The solid lines are least-squares fits to the data. Note the near-zero slope of the lower two lines, i.e., a film thickness independent of slit width, and the small increase in film thickness with decreasing surface separation for the top data set (the lower of the two lines is a fit to the filled squares).

Figure 4 shows a plot of $H_c$ vs $t_c$ with results from three separate experiments. For $t \leq 2$ nm $H_c$ is $12 \pm 1$ nm, similar to the $H_c$ found with nonpolar liquids and with ethanol at $p/p_0 < 0.99$ [14,15]. When $p/p_0 \ll 1$ (not shown), the jump separation decreases and in the limit of $p/p_0 = 0$ it is 3–5 nm, as expected from the van der Waals forces between mica surfaces across an inert atmosphere [15,20].

The disjoining pressure $\Pi$ of an adsorbed film on an isolated surface is given by

$$\Pi = -\frac{\partial G}{\partial t} = -\frac{kT}{v_m} \ln\left[\frac{p}{p_0}\right]. \tag{3}$$

If only dispersion forces act,

$$\Pi(t) = -\frac{A_{123}}{6\pi t^3}, \tag{4}$$

where $A_{123}$ is the Hamaker constant for solid and vapor across the adsorbed (liquid) film. Wetting implies that $A_{123}$ is negative and the disjoining pressure consequently positive and $\partial\Pi/\partial t < 0$ for all $t$. The presence of a second surface modifies Eq. (4) to [6,13]

$$-\Pi(H,t) = \frac{kT}{v_m} \ln[p/p_0] = \frac{A_{123}}{6\pi t^3} - \frac{A_{232}}{6\pi(H-2t)^3} + \frac{A_{123}}{6\pi(H-t)^3}. \tag{5}$$

Here $A_{232}$ is the Hamaker constant for the material in the adsorbed film interacting across vapor (vacuum) [see Fig. 1(a)]. The film loses its stability and coalesces when $(\partial\Pi/\partial t)(H,t) = 0$. This gives

$$\frac{A_{123}}{2t^4} + \frac{A_{232}}{(H-2t)^4} - \frac{A_{123}}{2(H-t)^4} = 0. \tag{6}$$

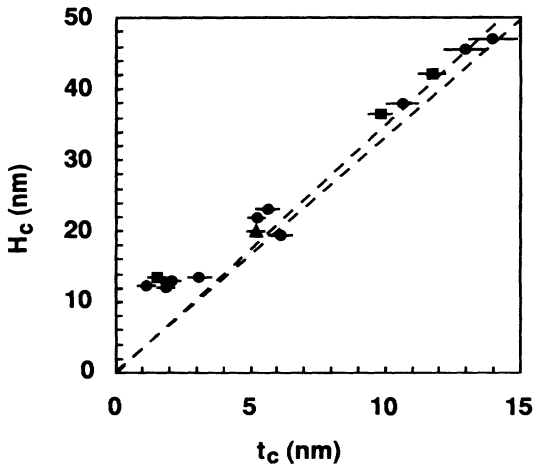


FIG. 4. Condensation separation $H_c$ as a function of film thickness at condensation $t_c$ for $t$-butanol films. The different symbols are the results of separate experiments. The error bars result from the standard deviation of the film thickness $t$ (see Fig. 3). The dashed lines are solutions to Eq. (6) with $A_{123} = -2 \times 10^{-20}$ J. $A_{323} = 5 \times 10^{-20}$ J (lower line) and $A_{123} = -3 \times 10^{-20}$ J, $A_{323} = 4 \times 10^{-20}$ J (upper line).

The last term may be neglected as a first approximation, in which case an analytic solution gives

$$t_c = \frac{H_c}{2 + (-2A_{232}/A_{123})/4}. \quad (7)$$

From this it is easily seen that $H_c \approx 3t_c$. The complete expression may be solved iteratively. The solutions are not strong functions of the exact values of the Hamaker constants. The best estimates of these, assuming that they are in the range of values for ethanol and short-chain alkanes, are $A_{232} = (4-5) \times 10^{-20}$ J [20] and $A_{123} = -(2-3) \times 10^{-20}$ J [2]. Using the complete expression [Eq. (6)] these values give a range of $H_c = 3.3t_c$ (lower line in Fig. 4) to $H_c = 3.5t_c$ (upper line). Given the errors in $t_c$ and the uncertainties in the Hamaker constants, the agreement for films >5 nm is excellent.

Note that the effects of retardation are expected to be negligible in this system. The predicted $H_c(t_c)$ hardly changes when both Hamaker constants in Eq. (5) are decreased in proportional amounts.

For thick films (≥5 nm) capillary condensation in a slit can be viewed as the coalescence of adsorbed films through the effect of van der Waals forces across the gap. For thin adsorbed layers the condensation separation is much larger than expected and the film-thickening model cannot explain the condensation. This is not surprising—van der Waals theory predicts the wrong functional form and underestimates the thickness of adsorbed layers in this regime [1,2].

I thank V. V. Yaminsky for numerous arguments and discussions, T. Sawkins and A. Hyde for technical assistance, T. Blake for a short visit, R. Evans for helpful comments, and L. E. McIntyre for her stimulating practical demonstrations.

[1] D. Beaglehole, E. Z. Radlinska, B. W. Ninham, and H. K. Christenson, Phys. Rev. Lett. **66**, 2084 (1991).

[2] D. Beaglehole and H. K. Christenson, J. Phys. Chem. **96**, 3395 (1992).

[3] J. E. Lane and T. H. Spurling, Aust. J. Chem. **33**, 231 (1980); J. E. Lane and T. H. Spurling, Aust. J. Chem. **34**, 1529 (1981).

[4] R. Evans and P. Tarazona, Phys. Rev. Lett. **52**, 557 (1984); R. Evans and U. Marini Bettolo Marconi, J. Chem. Phys. **86**, 7138 (1987).

[5] B. V. Derjaguin, Acta Physicochim. URSS **12**, 181 (1940).

[6] B. V. Derjaguin and N. V. Chauraev, J. Colloid Interface Sci. **54**, 157 (1976).

[7] D. D. Awschalom, J. Warnock, and M. W. Shafer, Phys. Rev. Lett. **57**, 1607 (1986); P. C. Ball and R. Evans, Europhys. Lett. **4**, 715 (1987); G. S. Heffelfinger, F. van Swol, and K. E. Gubbins, J. Chem. Phys. **89**, 5202 (1988).

[8] J. N. Israelachvili and G. E. Adams, J. Chem. Soc. Faraday Trans. 1 **74**, 975 (1978); J. L. Parker, H. K. Christenson, and B. W. Ninham, Rev. Sci. Instrum. **60**, 3135 (1989).

[9] L. R. Fisher and J. N. Israelachvili, J. Colloid Interface Sci. **80**, 528 (1981).

[10] H. K. Christenson, J. Colloid Interface Sci. **104**, 234 (1985).

[11] H. K. Christenson and C. E. Blom, J. Chem. Phys. **86**, 419 (1987).

[12] H. K. Christenson, J. Fang, and J. N. Israelachvili, Phys. Rev. B **39**, 11 750 (1989).

[13] M. L. Forcada, J. Chem. Phys. **98**, 638 (1993).

[14] H. K. Christenson and V. V. Yaminsky, Langmuir **9**, 2448 (1993).

[15] E. J. Wanless and H. K. Christenson, J. Chem. Phys. (to be published).

[16] B. V. Derjaguin, Kolloid Z. **69**, 155 (1934).

[17] *Handbook of Chemistry and Physics*, (CRC Press, Cleveland, OH, 1976), 57th ed.

[18] H. K. Christenson, J. Chem. Soc. Faraday Trans. 1 **80**, 1933 (1984).

[19] J. N. Israelachvili, J. Colloid Interface Sci. **44**, 259 (1973).

[20] J. N. Israelachvili, *Intermolecular and Surface Forces*, (Academic, London, 1991), 2nd ed.

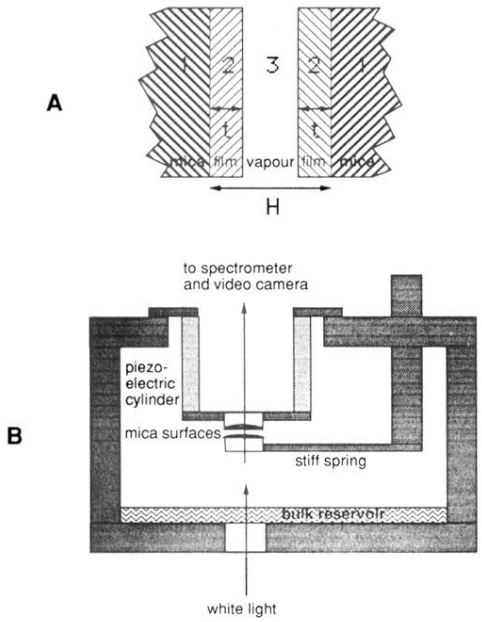


FIG. 1. Schematic depiction of (a) the "wet" slit and (b) the experimental setup.